Generated Pattern Current for Piezoelectric Domain Poling: Overcoming Static Electric Field Limitations in Ferroelectric Ceramic, Polymer Film, and Single Crystal Piezoelectric Activation

Ibrahim Karakoc
GigaPulse Energy, Izmir, Turkey
ibrahim@gigapulse.energy
PCT/TR2025/051176 | USPTO 19/298,223 | Priority date: July 23, 2025

Abstract

Generated Pattern Current (GPC) is a temporally structured electric field control framework derived from Jensen's inequality applied to nonlinear ferroelectric domain switching kinetics. This paper applies the GPC framework to piezoelectric domain poling across three principal material classes: lead zirconate titanate ferroelectric ceramics, polyvinylidene fluoride polymer films, and relaxor single crystal piezoelectrics. In each material class, conventional poling using a static direct current electric field imposes a fundamental dilemma: field levels below the coercive field produce incomplete domain switching and low piezoelectric coefficients, while field levels above the optimal range induce electrical breakdown, dielectric fatigue, and mechanical fracture that permanently degrade piezoelectric performance. The Landau-Khalatnikov domain switching kinetics governing ferroelectric polarization reversal are inherently nonlinear, and Jensen's inequality establishes that a temporally structured electric field at equal time-averaged intensity to a static field will produce different and exploitable domain switching outcomes. GPC addresses the static field dilemma by engineering a process-specific temporal field structure derived from the polarization hysteresis loop characteristics of each material: a primary switching phase that transiently exceeds the coercive field to maximize domain wall nucleation and propagation, followed by a consolidation phase that stabilizes switched domains without sustaining breakdown-risk field levels. The GP Lab reference platform implements the Dynamic Defined Pattern Charging algorithm for closed-loop GPC poling field control with real-time polarization monitoring. Experimental validation protocols are proposed for each material class.

Keywords: *Generated Pattern Current; GPC; Dynamic Defined Pattern Charging; DDPC; Piezoelectric Poling; Ferroelectric Domain Switching; Lead Zirconate Titanate; Polyvinylidene*

Fluoride; Single Crystal; Piezoelectric Coefficient; Jensen's Inequality; Landau-Khalatnikov Kinetics

1. Introduction

Piezoelectric materials convert mechanical deformation into electrical charge and, conversely, electrical stimulation into mechanical displacement. These bidirectional electromechanical transduction properties underpin a wide range of critical technologies: medical ultrasound imaging transducers, industrial nondestructive evaluation sensors, precision actuators for aerospace and semiconductor manufacturing, sonar systems for naval and oceanographic applications, energy harvesting devices for wireless sensor networks, and implantable medical devices [1, 2]. The global piezoelectric device market exceeds thirty billion dollars annually [3] and is projected to grow substantially as demand for precision sensors, actuators, and energy harvesting components in consumer electronics, electric vehicles, and medical diagnostics increases [3].

The functional piezoelectric properties of all commercially significant piezoelectric materials — ferroelectric ceramics, piezoelectric polymers, and relaxor single crystals — are not intrinsic to the as-fabricated material but must be induced through a manufacturing process called poling. In the as-sintered state, a ferroelectric ceramic such as lead zirconate titanate consists of crystallites containing ferroelectric domains — regions of uniform spontaneous polarization — oriented randomly throughout the bulk material. The random domain orientation produces a net macroscopic polarization of zero, and the material exhibits no useful piezoelectric response [4] [4]. Poling applies an external electric field sufficiently large to switch ferroelectric domains preferentially into alignment with the field direction, establishing a net remanent polarization that confers the piezoelectric properties required for device function.

The universal practice in piezoelectric manufacturing is to apply a static direct current electric field during poling. The material is immersed in a high-voltage insulating medium — typically silicon oil — and a constant electric field in the range of 1 to 4 kV/mm is applied at elevated temperature for durations of 5 to 30 minutes, after which the material is cooled to room temperature under the applied field [5, 6]. This static direct current poling convention, unchanged in its conceptual basis since the first systematic poling of lead zirconate titanate ceramics in the 1950s, imposes a

fundamental process dilemma that limits achievable piezoelectric coefficient values and production yield across all piezoelectric material classes.

The dilemma arises because the domain switching kinetics of ferroelectric materials are nonlinearly dependent on the applied field. Below the coercive field — the minimum field required to initiate domain switching — domain reversal is thermally activated and incomplete, producing a material with partially switched domains and a piezoelectric coefficient substantially below the saturation value [7]. At the coercive field, domain wall nucleation and propagation proceed rapidly, but the residence time of the applied field at the coercive field level must be balanced against the accumulating risk of dielectric fatigue and point defect redistribution that progressively reduce domain wall mobility and degrade long-term piezoelectric performance [8]. Above approximately twice the coercive field, the field exceeds the dielectric breakdown threshold of the material or its insulating medium, producing irreversible electrical discharge channels, mechanical crack propagation at grain boundaries, and permanent degradation of piezoelectric properties [9].

Generated Pattern Current (GPC), defined in patent filings PCT/TR2025/051176 and USPTO 19/298,223 [10], provides a systematic framework for resolving the static field dilemma through field delivery whose temporal structure is derived from first principles. GPC applies Jensen's inequality to the nonlinear Landau-Khalatnikov domain switching kinetics of ferroelectric materials, establishing that field structure — not merely field magnitude — determines domain switching outcomes when the polarization-field response function is nonlinear. This paper presents the first systematic application of the GPC framework to piezoelectric domain poling across three material classes: lead zirconate titanate ceramics (Section 3), polyvinylidene fluoride polymer films (Section 4), and relaxor single crystal piezoelectrics (Section 5). The GP Lab reference implementation is described in Section 6, and experimental validation protocols are proposed in Section 7.

2. Generated Pattern Current Framework Applied to Piezoelectric Poling

2.1 Landau-Khalatnikov Domain Switching Kinetics and Nonlinearity

Generated Pattern Current for piezoelectric poling is defined as $E(t) = A * s(t) + E0$, where $E(t)$ is the instantaneous applied electric field, $s(t)$ is the dimensionless shape function encoding the

temporal structure of the field, A is the amplitude scalar, and E0 is the DC offset. The time-averaged field is preserved by design, ensuring equal mean energy delivery to the material as a static field reference. Dynamic Defined Pattern Charging adjusts the scalar parameters A, E0, and duty cycle D in real time based on measured polarization current and impedance, while the engineered GPC form geometry of s(t) remains fixed throughout the poling process.

The theoretical foundation of GPC in piezoelectric poling is the Landau-Khalatnikov equation governing ferroelectric domain switching dynamics. The Landau-Khalatnikov equation describes the temporal evolution of polarization P under an applied field E as gamma * dP/dt = -dG/dP + E, where gamma is the kinetic coefficient governing domain wall mobility, and G(P) is the Landau-Ginzburg-Devonshire free energy functional expressed as G(P) = alpha*P^2 + beta*P^4 + delta*P^6, with coefficients alpha, beta, and delta characterizing the ferroelectric phase transition for the specific material [22]. The free energy functional is a polynomial of even powers of P, producing a double-well potential with minima at the positive and negative spontaneous polarization values Ps and -Ps. The switching trajectory from -Ps to +Ps under an applied field traverses this nonlinear potential landscape, making the polarization switching rate a highly nonlinear function of the applied field.

Jensen's inequality states that for a convex function f and a random variable x, the inequality f(E[x]) is less than or equal to E[f(x)] holds with strict inequality when f is strictly convex and x is non-degenerate. Applied to piezoelectric poling, where the domain switching rate function mapping applied field to polarization increment is nonlinear in the vicinity of the coercive field, an engineered field at equal mean intensity will produce a different time-averaged polarization switching outcome. The curvature of the switching rate function in the coercive field region — which transitions from thermally activated, sub-threshold switching at fields below the coercive field to collective domain wall avalanche behavior at fields above the coercive field — defines the Jensen gap available for exploitation through GPC form design [23].

The switching rate function exhibits strong convexity in the field range spanning from approximately 0.8 to 1.5 times the coercive field Ec. Below 0.8 Ec, switching is thermally dominated and the field-dependence is approximately exponential following the Merz law. Above 1.5 Ec, the switching rate approaches the domain wall velocity limit and the convexity decreases. GPC form design targets the 0.8 to 1.5 Ec range where the convexity is maximal, engineering a

primary switching phase that transiently elevates the field into this convex region to maximize the Jensen gain, followed by a consolidation phase at reduced field that stabilizes switched domains without sustaining the primary phase field level.

2.2 Limitations of Static Direct Current Field in Piezoelectric Poling

Static direct current poling fails to exploit ferroelectric nonlinearity in three distinct ways, each rooted in the fundamental conflict between a fixed field level and a switching process whose kinetic requirements change continuously throughout the poling duration.

The coercive field dilemma is the most direct consequence. A static field committed to a single level for the entire poling duration cannot satisfy two contradictory requirements simultaneously: the field must be high enough to initiate collective domain wall avalanche behavior, yet low enough to avoid accumulating dielectric fatigue and breakdown-risk exposure over the processing time. Below the coercive field the remanent d33 plateaus well short of its saturation value; at or above it, fatigue and defect redistribution progressively pin domain walls and degrade long-term piezoelectric performance.

The second limitation is grain boundary and interface inhomogeneity. In polycrystalline ceramics, the local coercive field varies between grains due to crystallographic orientation, grain size, and point defect concentration differences. A static field at the macroscopic coercive field level simultaneously over-poles some grains — subjecting them to fields well above their local coercive field — while under-poling others whose local coercive field exceeds the applied static field. This grain-to-grain heterogeneity in switching extent produces a distribution of local remanent polarization values that reduces the macroscopic piezoelectric coefficient below the single-crystal upper bound.

The third limitation is domain back-switching during cooling. Following static field poling, the applied field is maintained during cooling from the elevated poling temperature to room temperature. As the material cools, the coercive field increases — because domain wall mobility decreases with temperature — and the thermal stresses generated by cooling can drive back-switching of domains that were marginally switched near the coercive field during the hot poling phase. Static field poling cannot distinguish between domains switched reversibly — which will

back-switch on cooling — and domains switched irreversibly — which will retain their orientation — because both respond identically to a static field.

Table 1. Comparison of static direct current and GPC poling across three piezoelectric material classes: process parameters, principal limitations, and predicted performance gains.

Parameter	PZT Ceramic (DC)	PZT Ceramic (GPC)	PVDF Film (DC)	PVDF Film (GPC)	PMN-PT Crystal (DC / GPC)
Poling field	1.5–2.0 Ec (fixed)	2.0 Ec primary 0.7 Ec consol.	50–100 MV/m (fixed)	1.6 Ec primary 0.5 Ec propag.	DC: 0.3–0.7 kV/mm GPC: multi-step
Field exposure at breakdown risk	Full duration (10–30 min)	Primary phase only (~30% duty)	Full duration (20–40 min)	Primary phase only (~25% duty)	Single high-field event → GPC: staged
Domain switching mechanism	Collective wall avalanche (static)	Jensen-gap exploited at Ec	Nucleation-limited (static)	Nucleation burst + propagation	Phase rotation (static compromise)
Grain/film heterogeneity	Over/under-poling across grains	DDPC adapts A in real time	Breakdown at thick/defect sites	Reduced total breakdown exposure	Crystal variance detected by permitt.
Cooling phase control	Fixed field (back-switch risk)	DDPC tracks Ec(T) continuously	Fixed field (chain relax. risk)	Low-field stabilization	GPC: permittivity-guided hold field
Predicted d33 gain vs DC	—	+15 to +30% (LK convexity)	—	+20 to +40% (nucleation kinetics)	GPC: +10 to +20% (phase decoupling)
Breakdown / yield impact	Baseline yield	Equal or better yield (less fatigue)	Baseline yield (~70–85%)	Improved yield (less peak exposure)	GPC: lower fracture risk at phase boundary
Energy input (mean field)	Reference	Equal to DC reference	Reference	Equal to DC reference	Equal to DC reference

LK = Landau-Khalatnikov; Ec = coercive field; DDPC = Dynamic Defined Pattern Charging; PMN-PT = lead magnesium niobate-lead titanate; permitt. = dielectric permittivity. Orange columns: static DC; green columns: GPC; purple column: combined comparison for single crystals.

3. Generated Pattern Current Poling of Lead Zirconate Titanate Ferroelectric Ceramics

3.1 Domain Switching Physics and Static Field Limitations in Lead Zirconate Titanate

Lead zirconate titanate is the dominant commercial piezoelectric ceramic, with piezoelectric coefficients d33 in the range of 200 to 600 pC/N depending on composition, dopant type, and

poling conditions [11]. The tetragonal phase of lead zirconate titanate near the morphotropic phase boundary exhibits particularly high piezoelectric response due to the proximity of multiple energetically equivalent polarization states that facilitate domain wall motion under applied field. The coercive field of commercial soft lead zirconate titanate compositions ranges from 0.5 to 1.5 kV/mm at room temperature, decreasing by approximately a factor of three at elevated poling temperatures of 100 to 150 degrees Celsius [12].

Static direct current poling of lead zirconate titanate ceramics has been extensively studied and optimized through empirical parameter screening — poling field, temperature, and duration — for each specific composition [6, 13]. The empirical optimization approach has identified conditions that produce consistent d33 values for given compositions, but the static field convention places a ceiling on achievable d33 that is not composition-limited but process-limited. The ceiling arises because the optimal static field — the field that maximizes d33 without inducing breakdown or fatigue — lies in a narrow window around 1.5 to 2.0 times the coercive field. Below this window, domain switching is incomplete. Above this window, the risk of dielectric breakdown increases rapidly with field level for the typical processing times of 10 to 30 minutes.

Recent experimental investigations have demonstrated that time-varying field protocols — including high-temperature poling above the Curie temperature, multiple poling cycles at the coercive field, and pulsed field approaches — can produce d33 values 15 to 40 percent higher than optimized static field poling for the same composition [14, 15]. These results confirm that the temporal structure of the applied field, not merely its magnitude, determines the achievable piezoelectric coefficient. GPC provides the first-principles framework for systematically designing the optimal temporal field structure [24, 25, 26] from the Landau-Khalatnikov kinetics and polarization hysteresis loop of the specific lead zirconate titanate composition.

3.2 Generated Pattern Current Form Design for Lead Zirconate Titanate Poling

The GPC form for lead zirconate titanate poling is derived from three material parameters that can be measured directly from the polarization-electric field hysteresis loop of the specific composition at the target poling temperature: the coercive field Ec, the saturation polarization Ps, and the remanent polarization Pr. These three parameters fully characterize the double-well free energy functional of the Landau-Ginzburg-Devonshire model and define the shape of the switching rate function.

The GPC primary switching phase is set at a field amplitude of 1.8 to 2.2 Ec — above the coercive field to maximize domain wall nucleation density and propagation velocity, but below the dielectric breakdown threshold that typically occurs above 3 to 4 Ec for commercial lead zirconate titanate compositions in silicon oil insulation. The primary phase duration is calibrated to the domain wall propagation time constant: long enough to complete collective domain switching across the primary grain population, but short enough to prevent accumulation of dielectric fatigue at the elevated field level. The domain wall propagation time constant is estimated from the switching current transient measured at the onset of the primary phase.

The GPC consolidation phase follows each primary switching phase at a reduced field of 0.6 to 0.8 Ec — below the coercive field to prevent back-switching of newly oriented domains, but above zero to maintain a restoring force that stabilizes the switched domain configuration against thermal fluctuations at the elevated poling temperature. The consolidation phase duration is matched to the domain stabilization time constant: the characteristic time for newly switched domains to pin at grain boundaries and point defect sites that prevent back-switching.

The temporal alternation between primary switching and consolidation phases exploits the Jensen inequality in the coercive field transition region: at equal time-averaged field, the primary phase drives more domain switching per unit time than a static field at the average level, because the switching rate function is convex in the coercive field transition region. The net result is a higher time-averaged domain switching rate and a higher final remanent polarization — and therefore a higher d33 — at equal mean energy input.

The GPC form for lead zirconate titanate further incorporates a temperature-coupled field adjustment through the DDPC algorithm. As the material cools from the elevated poling temperature under the GPC form, the coercive field increases. DDPC tracks the real-time polarization current to detect the shift in coercive field with temperature and adjusts the scalar amplitude A to maintain the ratio of primary phase amplitude to instantaneous coercive field within the optimal 1.8 to 2.2 Ec range throughout the cooling phase, preventing domain back-switching that degrades the room-temperature d33.

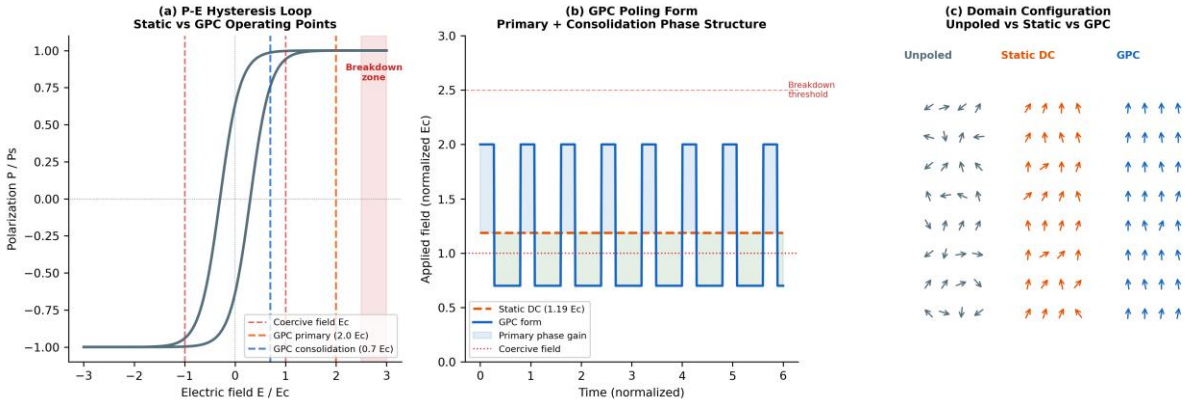

Figure 1. Lead zirconate titanate polarization-electric field hysteresis loop showing the Landau-Khalatnikov nonlinearity exploited by the GPC poling framework. (a) Static direct current field at a fixed operating point — below optimal: incomplete switching; above optimal: breakdown risk. (b) GPC primary switching phase at 2.0 Ec and consolidation phase at 0.7 Ec, alternating at the domain wall propagation time constant. The Jensen gap between GPC and static field remanent polarization at equal mean field is indicated. (c) Schematic domain configuration: random in unpoled material, partially aligned under static field, highly aligned under GPC form.

4. Generated Pattern Current Poling of Polyvinylidene Fluoride Polymer Films

4.1 Beta-Phase Crystallinity and Poling Physics in Polyvinylidene Fluoride

Polyvinylidene fluoride is a semi-crystalline polymer with four principal crystalline phases — alpha, beta, gamma, and delta — of which the beta phase is the only strongly piezoelectric phase due to its all-trans chain conformation that produces a large net dipole moment per unit cell [17]. The as-processed polyvinylidene fluoride film typically contains predominantly the non-polar alpha phase; converting the polymer to the beta phase and then orienting the beta-phase dipoles through poling are the two sequential steps required to produce a functional piezoelectric film [18].

The poling of polyvinylidene fluoride differs physically from ceramic poling in two important ways. First, the dielectric breakdown field of polyvinylidene fluoride is substantially lower than lead zirconate titanate — typically 50 to 150 MV/m for polymer films versus 300 to 600 MV/m for dense ceramics — making the margin between optimal poling field and breakdown threshold considerably narrower. Second, the domain switching mechanism in polyvinylidene fluoride involves reorientation of fluorine-carbon-fluorine bond angles along the polymer chain backbone rather than ionic displacement, making the domain switching kinetics more sensitive to chain mobility and therefore more strongly temperature-dependent than ceramic domain switching.

The static field poling dilemma in polyvinylidene fluoride is consequently more severe than in ceramics. The optimal static field for polyvinylidene fluoride poling is typically 50 to 100 MV/m — close to the breakdown threshold — and the poling process must be conducted at temperatures of 60 to 100 degrees Celsius to enhance chain mobility sufficiently for effective dipole reorientation. The narrow operating window between optimal poling field and breakdown threshold means that film inhomogeneities — thickness variations, surface defects, trapped charge regions — routinely cause localized breakdown under static field poling, reducing production yield and limiting the achievable d33.

4.2 Generated Pattern Current Form Design for Polyvinylidene Fluoride Poling

The GPC form for polyvinylidene fluoride poling is derived from the polarization-field switching characteristics of the specific film grade at the target poling temperature. The switching kinetics of polyvinylidene fluoride in the vicinity of the coercive field follow a nucleation-limited switching model in which the switching rate is an exponential function of the applied field, making the switching rate function highly convex in the coercive field transition region and therefore particularly favorable for GPC exploitation.

The primary switching phase of the polyvinylidene fluoride GPC form applies a field of 1.5 to 1.8 times the film coercive field for a duration matched to the nucleation time constant — the characteristic time for beta-phase dipole nuclei to form and initiate chain reorientation. This duration is typically in the range of milliseconds to seconds, substantially shorter than the minutes-long static field poling exposure that accumulates the thermal and electrical damage responsible for film degradation. The consolidation phase at 0.4 to 0.6 times the coercive field allows the initiated dipole reorientation to propagate along the polymer chain without sustaining the breakdown-risk primary phase field level.

The key advantage of GPC for polyvinylidene fluoride poling is the decoupling of nucleation driving force from total exposure time at elevated field. Under static field poling, achieving high nucleation density requires a high field that must be sustained for an extended period to complete chain reorientation throughout the film thickness, accumulating total breakdown exposure proportional to field times duration. GPC concentrates the high-field exposure into brief primary switching phases that maximize nucleation density, while the consolidation phases allow chain reorientation to propagate under low-field stabilization. The total exposure time at breakdown-risk

field levels is reduced by the primary phase duty cycle — typically 20 to 40 percent — while the nucleation density achieved is equal to or greater than static field poling at the same average field.

For polyvinylidene fluoride films incorporating piezoelectric ceramic particles in composite configurations, the GPC form must account for the difference in coercive field between the polymer matrix and the ceramic inclusions. DDPC monitors the composite polarization current to detect contributions from polymer chain switching and ceramic domain switching at their respective coercive fields, enabling the GPC form to be adapted in real time to address both switching mechanisms optimally.

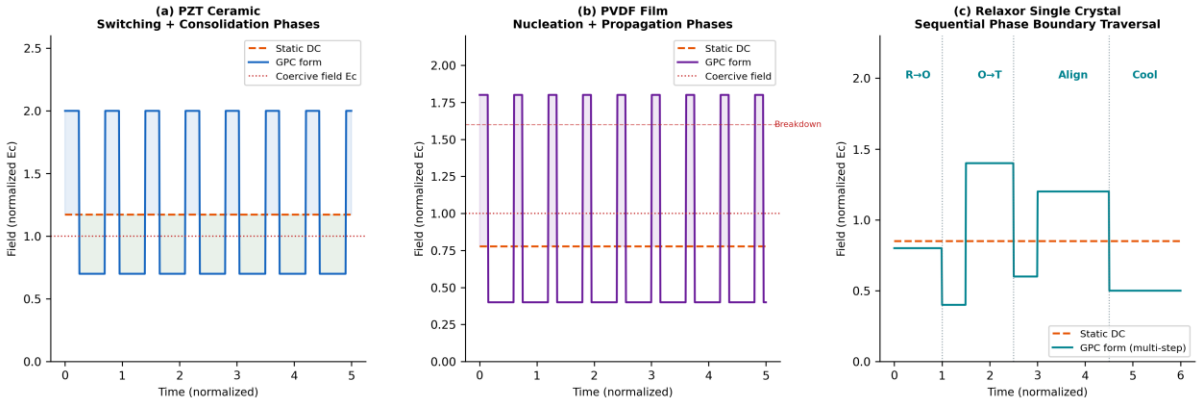

Figure 2. Process-specific GPC forms for the three piezoelectric material classes. (a) Lead zirconate titanate ceramic GPC form: primary switching phase at 2.0 Ec and consolidation phase at 0.7 Ec, with DDPC temperature-coupled amplitude adjustment during cooling. (b) Polyvinylidene fluoride polymer GPC form: high-field nucleation phase matched to chain reorientation nucleation time constant, low-field propagation phase for chain reorientation completion. (c) Relaxor single crystal GPC form: engineered phase boundary traversal sequence targeting morphotropic phase boundary polarization rotation. All forms preserve time-averaged field equal to the static direct current reference.

5. Generated Pattern Current Poling of Relaxor Single Crystal Piezoelectrics

5.1 Phase Boundary Polarization and Poling Physics in Relaxor Single Crystals

Relaxor single crystal piezoelectrics — principally lead magnesium niobate-lead titanate and lead indium niobate-lead magnesium niobate-lead titanate — exhibit piezoelectric coefficients d33 in the range of 1500 to 3000 pC/N, an order of magnitude above lead zirconate titanate ceramics, making them the preferred material for high-performance medical ultrasound transducers, sonar projectors, and precision actuators [19]. The exceptional piezoelectric response of relaxor single

crystals arises from the proximity of the morphotropic phase boundary — the composition range where rhombohedral and tetragonal phases coexist — and the associated polarization rotation mechanism in which the applied field rotates the spontaneous polarization vector through energetically favorable intermediate phase states rather than reversing individual domain orientations.

The poling of relaxor single crystals is considerably more process-sensitive than ceramic poling because the polarization rotation mechanism is strongly anisotropic and temperature-sensitive. The optimal poling configuration for maximum d33 in lead magnesium niobate-lead titanate crystals is the [001] crystallographic direction, which accesses the highest-symmetry polarization rotation pathway through rhombohedral-orthorhombic-tetragonal phase intermediates [20]. Achieving full polarization rotation in the [001] direction requires a specific sequence of field amplitudes and temperatures that navigates the phase boundary landscape — insufficient field leaves the polarization in intermediate phase states with lower d33, while excessive field induces cracking of the mechanically brittle single crystal or permanent phase destabilization.

Static direct current poling of relaxor single crystals is therefore particularly sensitive to field level, with optimal d33 values achievable only within a narrow field window of approximately 0.3 to 0.7 kV/mm at temperatures of 100 to 150 degrees Celsius. The narrow optimal window reflects the phase boundary topology: the transition from the rhombohedral to the orthorhombic intermediate phase is sharp, and static fields in the transition region either fail to complete the transition or overshoot it into an undesired tetragonal domain configuration that reduces d33.

5.2 Generated Pattern Current Form Design for Relaxor Single Crystal Poling

The GPC form for relaxor single crystal poling is derived from the free energy landscape of the specific crystal composition in the vicinity of the morphotropic phase boundary. Unlike ceramic and polymer poling, where the GPC form targets the coercive field nonlinearity of a single switching transition, the single crystal GPC form targets the sequential phase boundary transitions of the polarization rotation pathway.

The GPC form for lead magnesium niobate-lead titanate [001] poling consists of a multi-phase temporal structure matched to the phase boundary transition sequence: a rhombohedral-to-orthorhombic transition phase at a field amplitude calibrated to drive polarization rotation through

the first phase boundary, followed by a stabilization phase at reduced field that consolidates the orthorhombic intermediate polarization state, followed by an orthorhombic-to-tetragonal rotation phase at a higher field amplitude that completes the rotation to the [001]-aligned tetragonal state. Each phase boundary transition is a separate nonlinear switching event with its own free energy barrier and kinetic time constant, and the GPC form engineering addresses each transition as a distinct step in a sequential nonlinear process.

This multi-step GPC form structure provides a fundamental advantage over static field poling for single crystals: it decouples the field requirements of successive phase transitions that have different optimal field amplitudes. Static field poling must set a single field level that represents a compromise between the under-field for one transition and the over-field for the next. GPC engineering of a sequential phase-boundary-matched temporal structure eliminates this compromise by addressing each phase transition with its optimal field amplitude and duration.

The DDPC algorithm for single crystal poling monitors the real-time dielectric permittivity measured at a low-amplitude probe frequency superimposed on the GPC form. The dielectric permittivity of relaxor single crystals exhibits sharp anomalies at each phase boundary crossing, providing a real-time signature of the polarization state that GP Lab uses to confirm completion of each phase transition before initiating the next GPC phase. This real-time phase boundary detection capability is not available with static field poling and enables adaptive adjustment of the GPC form to account for crystal-to-crystal variations in phase boundary field and temperature.

6. GP Lab Reference Implementation

6.1 System Architecture for Piezoelectric Poling Applications

The GP Lab system provides a reference implementation of the GPC framework for piezoelectric poling research and process development. GP Lab interfaces with any standard high-voltage source through its output control interface, requiring only polarization current and voltage measurement at the poling electrode terminals. The existing poling fixture — electrode plates, silicon oil bath, temperature-controlled oven — requires no modification.

GP Lab connects to the high-voltage Power Source input terminals and transmits E_ref(t) control signals specifying the instantaneous poling field setpoint. The Power Source applies the

commanded field to the piezoelectric sample through the poling electrodes. The sample connects to the Power Source only — GP Lab is the control and intelligence layer, not a power source. Feedback signals including polarization current I(t), electrode voltage V(t), and oven temperature T(t) return from the Power Source measurement circuits to GP Lab. GP Lab computes the instantaneous polarization P from the time-integral of the polarization current after capacitive baseline subtraction, the domain switching rate dP/dt, the effective coercive field Ec from the polarization current peak, and the dielectric permittivity from the small-signal impedance in real time. The DDPC algorithm updates the scalar parameters A, E0, and D to maintain the GPC primary phase amplitude at the target ratio to the measured instantaneous coercive field throughout the poling and cooling sequence.

6.2 Process-Specific Generated Pattern Current Form Deployment

For each piezoelectric material class, GP Lab executes a process-specific GPC form engineered from the polarization-field hysteresis loop parameters of the specific material at the target poling temperature.

For lead zirconate titanate, the firmware configuration specifies the primary phase amplitude ratio to Ec, the primary and consolidation phase durations as multiples of the measured domain wall propagation time constant, and the DDPC temperature-coupling law relating amplitude adjustment to measured oven temperature during cooling.

For polyvinylidene fluoride, the configuration carries the primary nucleation phase amplitude, the nucleation time constant extracted from the polarization current transient at field onset, and the duty cycle calibrated to the breakdown voltage margin of the specific film grade and thickness.

For relaxor single crystals, the multi-step phase boundary traversal sequence — rhombohedral-orthorhombic amplitude, stabilization amplitude, and orthorhombic-tetragonal amplitude — together with the permittivity anomaly threshold signatures that trigger DDPC phase advancement in real time.

All GPC forms preserve the time-averaged electric field equal to the static direct current design specification, ensuring that total energy delivery to the piezoelectric material is equal to the static field reference for direct comparison of d33 outcomes.

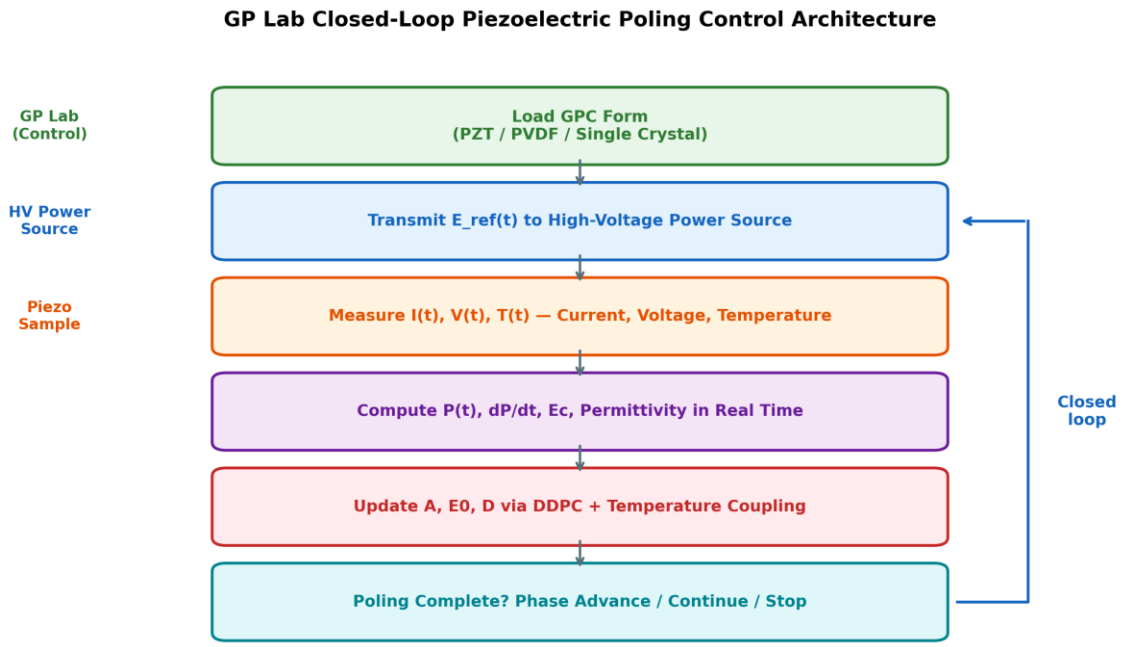

Figure 3. GP Lab closed-loop piezoelectric poling control architecture. GP Lab loads the process-specific GPC form, transmits E_ref(t) to the high-voltage power source, measures polarization current I(t) and electrode voltage V(t), computes instantaneous polarization P, domain switching rate dP/dt, coercive field Ec, and dielectric permittivity in real time, and updates scalar parameters A, E0, and D via the DDPC algorithm without modifying the engineered GPC form geometry. Temperature feedback from the oven enables DDPC temperature-coupled amplitude adjustment during cooling.

7. Experimental Validation Framework

The GPC framework for piezoelectric poling generates specific, testable predictions for each material class. The following validation protocols are proposed for researchers using standard ferroelectric characterization equipment and the GP Lab reference platform.

For lead zirconate titanate ceramic validation: prepare commercial soft lead zirconate titanate discs with sputtered gold electrodes at a thickness appropriate for the target poling field range. Measure the polarization-field hysteresis loop at the target poling temperature of 100 degrees Celsius using a Sawyer-Tower circuit to extract Ec, Ps, and Pr for the specific batch. Pole a set of ten discs under static direct current at 2.0 Ec for 10 minutes and measure d33 by Berlincourt meter after 24-hour room temperature stabilization. Pole a matched set of ten discs under the process-specific GPC form with identical time-averaged field of 2.0 Ec and total poling duration of 10 minutes using GP

Lab. Key metrics: mean d33 (GPC prediction: 15 to 30 percent higher than static field based on Landau-Khalatnikov convexity analysis at the specific Ec and Ps values); d33 coefficient of variation across the set (GPC prediction: lower than static field, reflecting more complete domain switching with reduced grain-to-grain heterogeneity); and dielectric loss at 1 kHz after poling (GPC prediction: equal or lower than static field, indicating reduced dielectric fatigue).

For polyvinylidene fluoride film validation: prepare commercial beta-phase polyvinylidene fluoride film of 28 micrometer thickness with chromium-gold electrodes. Measure the switching current transient under a field step from zero to 60 MV/m to extract the nucleation time constant for the specific film grade. Pole a set of ten film samples under static direct current at 80 MV/m for 30 minutes at 80 degrees Celsius and measure d33. Pole a matched set under the process-specific GPC form with identical mean field and duration using GP Lab. Key metrics: mean d33 (GPC prediction: 20 to 40 percent higher based on nucleation kinetics convexity analysis); breakdown failure rate (GPC prediction: lower than static field due to reduced total exposure time at breakdown-risk field levels); and beta-phase crystallinity by Fourier transform infrared spectroscopy (GPC prediction: equal or higher than static field).

For relaxor single crystal validation: prepare lead magnesium niobate-lead titanate single crystal platelets oriented in the [001] direction with gold electrodes at a thickness consistent with the target phase boundary traversal field. Measure the temperature-field phase diagram using in-situ dielectric permittivity mapping to identify the rhombohedral-orthorhombic and orthorhombic-tetragonal phase boundary fields at the target poling temperature. Pole under static direct current at the standard protocol and measure d33. Pole under the multi-step GPC form using GP Lab with real-time permittivity phase boundary detection. Key metrics: d33 (GPC prediction: 10 to 20 percent higher than static field based on sequential phase transition decoupling); permittivity uniformity across the crystal area (GPC prediction: higher uniformity, reflecting more complete morphotropic phase boundary polarization rotation); and mechanical integrity (GPC prediction: equal or superior, as the multi-step field structure avoids the single high-field event that most commonly initiates single crystal fracture).

8. Discussion

The application of the GPC framework to piezoelectric domain poling reveals that the static direct current convention adopted in piezoelectric manufacturing since the 1950s is not a theoretically optimal process but a practical default determined by the capabilities of early high-voltage power supply technology. The Landau-Khalatnikov domain switching kinetics governing ferroelectric polarization reversal are inherently nonlinear, and Jensen's inequality establishes that field temporal structure at equal mean intensity will produce superior domain switching outcomes in all three material classes analyzed in this paper.

The relationship between GPC poling and the emerging experimental literature on time-varying field protocols requires careful positioning. High-temperature poling above the Curie temperature [14], multiple field cycle poling [15], pulse poling showing d33 increases above 65 percent in relaxor single crystals relative to direct current [16], and the recent discovery that alternating current fields can achieve depoling not possible with direct current [21] all represent experimental observations that the field structure — not merely its magnitude — determines piezoelectric poling outcomes. These observations reflect the Jensen inequality applied to the Landau-Khalatnikov nonlinearity, operating without systematic optimization of the field structure for the specific material. GPC form design derived analytically from the measured polarization hysteresis loop parameters enables systematic optimization rather than empirical parameter variation, providing a principled framework for explaining these experimental observations and predicting optimal field structures for new compositions.

The GPC framework does not require new electrode materials, new poling fixtures, or new dielectric insulation systems. The process-specific GPC form is delivered to any existing high-voltage power supply as a field reference signal through GP Lab's control interface. This enables GPC technology to be deployed as a software and control system upgrade to existing poling equipment without capital investment in new process hardware. The productivity benefit — higher d33 at equal process time and energy, or equal d33 at reduced process time and energy — is achievable immediately from the control layer upgrade.

The most significant industrial opportunity for GPC poling may be in the manufacturing of polyvinylidene fluoride flexible sensors and energy harvesters, where the narrow margin between optimal poling field and breakdown threshold limits production yield under static field conditions. Reducing breakdown failure rate while simultaneously improving d33 would directly improve the

economics of flexible piezoelectric device manufacturing — a rapidly growing sector driven by demand for wearable health monitoring devices, smart textiles, and implantable biosensors. The GPC framework provides a systematic basis for optimizing the temporal field structure to simultaneously maximize nucleation density and minimize breakdown exposure, a combination not achievable with any static field protocol.

9. Conclusion

This paper has established the Generated Pattern Current framework as a unified first-principles basis for advancing piezoelectric domain poling across three material classes: lead zirconate titanate ferroelectric ceramics, polyvinylidene fluoride polymer films, and relaxor single crystal piezoelectrics. The common foundation is Jensen's inequality applied to the nonlinear Landau-Khalatnikov domain switching kinetics: an engineered temporal field at equal mean intensity to a static field produces superior domain switching outcomes whenever the switching rate function is nonlinear in the applied field.

For lead zirconate titanate ceramics, GPC provides primary switching and consolidation phase alternation that maximizes domain wall nucleation density while minimizing dielectric fatigue at the primary phase field level, achieving higher remanent polarization and d33 at equal mean energy input. For polyvinylidene fluoride films, GPC decouples nucleation driving force from total breakdown exposure time, enabling higher beta-phase dipole alignment at reduced breakdown failure probability. For relaxor single crystals, GPC provides sequential phase boundary traversal with real-time permittivity detection, decoupling the field requirements of successive polarization rotation transitions and enabling more complete [001]-direction polarization alignment.

The experimental validation protocols proposed in Section 7 provide a roadmap for the piezoelectric materials research community to evaluate these predictions using standard ferroelectric characterization equipment and the GP Lab reference platform. The patent filings PCT/TR2025/051176 and USPTO 19/298,223 protect the core GPC architecture while the complete scientific framework is disclosed here to enable independent experimental evaluation and adoption by the piezoelectric manufacturing community.

References

[1] Uchino K. Piezoelectric actuators 2010: Key configurations and high-power applications. J Electroceram. 2010;25(2-4):49-56.

[2] Park SE, Shrout TR. Ultrahigh strain and piezoelectric behavior in relaxor based ferroelectric single crystals. J Appl Phys. 1997;82(4):1804-1811.

[3] Grand View Research. Piezoelectric Devices Market Size Report. San Francisco: Grand View Research; 2024.

[4] Jaffe B, Cook WR, Jaffe H. Piezoelectric Ceramics. London: Academic Press; 1971.

[5] Berlincourt D. Piezoelectric crystals and ceramics. In: Mattiat OE, ed. Ultrasonic Transducer Materials. New York: Plenum Press; 1971:63-124.

[6] Akdogan EK, Allahverdi M, Safari A. Piezoelectric composites for sensor and actuator applications. IEEE Trans Ultrason Ferroelectr Freq Control. 2005;52(5):746-775.

[7] Merz WJ. Domain formation and domain wall motions in ferroelectric BaTiO3 single crystals. Phys Rev. 1954;95(3):690-698.

[8] Scott JF. Applications of modern ferroelectrics. Science. 2007;315(5814):954-959.

[9] Gao H, Zhang TY, Tong P. Local and global energy release rates for an electrically yielded crack in a piezoelectric ceramic. J Mech Phys Solids. 1997;45(4):491-510.

[10] Karakoc I. Generated Pattern Current system and method. PCT/TR2025/051176; USPTO 19/298,223. Priority date: July 23, 2025.

[11] Noheda B, Cox DE, Shirane G, et al. Stability of the monoclinic phase in the ferroelectric perovskite PbZr1-xTixO3. Phys Rev B. 2001;63(1):014103.

[12] Haun MJ, Furman E, Jang SJ, et al. Thermodynamic theory of PbTiO3. J Appl Phys. 1987;62(8):3331-3338.

[13] Hall DA, Daniel L, Watson M, Condie A, Comyn TP. Domain switching and shear-mode piezoelectric response induced by cross-poling in polycrystalline ferroelectrics. J Appl Phys. 2024;136(19):194101.

[14] Liu X, Zhang Y, Tang M, et al. Enhancing electromechanical properties of PZT-based ceramics by high-temperature poling. ACS Appl Mater Interfaces. 2023;15(4):5872-5881.

[15] Maurya D, Zhou Y, Yan Y, Priya S. Synthesis mechanism of grain-oriented lead-free piezoelectric Na0.5Bi0.5TiO3-BaTiO3 ceramics. J Mater Chem C. 2013;1(11):2102-2111.

[16] Mervosh MW, Jones H, Arguelles AP, Trolier-McKinstry S, Randall CA. A comparative consideration of the link between poling procedure, induced damage, and piezoelectric response in perovskite ferroelectrics. J Appl Phys. 2025;137(24):244102.

[17] Lovinger AJ. Ferroelectric polymers. Science. 1983;220(4602):1115-1121.

[18] Bauer F. PVDF shock sensors: applications to polar materials and high explosives. IEEE Trans Ultrason Ferroelectr Freq Control. 2000;47(6):1448-1454.

[19] Zhang S, Li F. High performance ferroelectric relaxor-PbTiO3 single crystals: status and perspective. J Appl Phys. 2012;111(3):031301.

[20] Davis M, Damjanovic D, Setter N. Electric-field-, temperature-, and stress-induced phase transitions in relaxor ferroelectric single crystals. Phys Rev B. 2006;73(1):014115.

[21] Kim HP, Zhang MH, Wang B, et al. Electrical de-poling and re-poling of relaxor-PbTiO3 piezoelectric single crystals without heat treatment. Nat Commun. 2024;15:6420.

[22] Lines ME, Glass AM. Principles and Applications of Ferroelectrics and Related Materials. Oxford: Clarendon Press; 1977.

[23] Damjanovic D. Ferroelectric, dielectric and piezoelectric properties of ferroelectric thin films and ceramics. Rep Prog Phys. 1998;61(9):1267-1324.

[24] Zhang S, Xia R, Lebrun L, Anderson D, Shrout TR. Piezoelectric materials for high power, high temperature applications. Mater Lett. 2005;59(27):3471-3475.

[25] Chu BJ, Chen DR, Li GR, Yin QR. Electrical properties of Na1/2Bi1/2TiO3-BaTiO3 ceramics. J Eur Ceram Soc. 2002;22(13):2115-2121.

[26] Saito Y, Takao H, Tani T, et al. Lead-free piezoceramics. Nature. 2004;432(7013):84-87.

[26] Karakoc I. Generated Pattern Current in Battery Formation: A Jensen Inequality Framework. J Power Sources. 2026. SSRN 6392399.

[27] Karakoc I. Generated Pattern Current in Battery Charging Optimization. J Power Sources. 2026. SSRN 6392719.

[28] Karakoc I. Generated Pattern Current for Fuel Cell Conditioning. Int J Hydrogen Energy. 2026. SSRN 6427558.

[29] Karakoc I. Generated Pattern Current in Electroplating. J Appl Electrochem. 2026. SSRN 6439004.

[30] Karakoc I. Generated Pattern Current in Anodizing. Electrochim Acta. 2026. SSRN 6442358.

[31] Karakoc I. Generated Pattern Current for Neurostimulation. Med Biol Eng Comput. 2026. SSRN 6490398.

[32] Karakoc I. Generated Pattern Current in Impressed Current Cathodic Protection. Corros Sci. 2026. SSRN 6495839.

[33] Karakoc I. Generated Pattern Current in Electrochemical Water Treatment. Desalination. 2026. SSRN 6486959.

Acknowledgments

The GPC-based anodizing protocol is protected under PCT/TR2025/051176 and USPTO Application No. 19/298,223. The author is the named inventor. No external funding was received for the preparation of this manuscript.

Declaration of Competing Interest

Ibrahim Karakoc holds the intellectual property and commercial rights related to the Generated Pattern Current (GPC) and Dynamic Defined Pattern Charging (DDPC) technology described in this paper.

Data Availability

Data will be made available on request.

Declaration on Use of AI Writing Assistance

The author used an AI language assistant for manuscript preparation and English language refinement. The author is fully responsible for all scientific content and conclusions presented in this manuscript.